

Conversion of CH₄/CO₂ by a nanosecond repetitively pulsed discharge

This content has been downloaded from IOPscience. Please scroll down to see the full text.

2016 J. Phys. D: Appl. Phys. 49 075602

(<http://iopscience.iop.org/0022-3727/49/7/075602>)

View [the table of contents for this issue](#), or go to the [journal homepage](#) for more

Download details:

IP Address: 194.27.18.18

This content was downloaded on 01/02/2016 at 05:19

Please note that [terms and conditions apply](#).

Conversion of CH₄/CO₂ by a nanosecond repetitively pulsed discharge

M Scapinello¹, L M Martini², G Dilecce^{2,3} and P Tosi²

¹ CNR-IMCB, UOS Trento, via Sommarive 14, Trento I-38123, Italy

² Department of Physics, University of Trento, via Sommarive 14, Trento I-38123, Italy

³ CNR-NANOTEC, via Amendola 122/D4, Bari I-70126, Italy

E-mail: paolo.tosi@unitn.it

Received 5 November 2015, revised 15 December 2015

Accepted for publication 18 December 2015

Published 29 January 2016



Abstract

A possible way to store both renewable energy and CO₂ in chemical energy is to produce value-added chemicals and fuels starting from CO₂ and green electricity. This can be done by exploiting the non-equilibrium properties of gaseous electrical discharges. Discharges, in addition, can be switched on and off quickly, thus being suitable to be coupled with an intermittent energy source. In this study, we have used a nanosecond pulsed discharge to dissociate CO₂ and CH₄ in a 1:1 mixture at atmospheric pressure, and compared our results with literature data obtained by other discharges. The main products are CO, H₂, C₂H₂, water and solid carbon. We estimate an energy efficiency of 40% for syngas (CO and H₂) production, higher if other products are also considered. Such values are among the highest compared to other discharges, and, although not very high on an absolute scale, are likely improvable via possible routes discussed in the paper and by coupling to the discharge a heterogeneous catalysis stage.

Keywords: dry reforming, CO₂, CH₄, energy storage, nanosecond pulsed discharge

(Some figures may appear in colour only in the online journal)

1. Introduction

Satisfying the world's increasing energy demand while reducing negative impacts on the Earth's climate is a paramount challenge in present days. In the past 10 years, the energy scenario has changed radically due to the increased availability of natural gas, not to say coal. The present established reserves of natural gas of about 186 trillion cubic meters compare with an annual (2013) world consumption of about 3348 billion cubic meters, which means they will meet the (2013) gas demand for at least 55 years [1]. In addition, unconventional gas sources, thought to be currently not exploited, might play an increasing role in the future. However, a main problem with natural gas is its low energy density in comparison with liquid fuel. As an example, in order to be shipped overseas, natural gas must be cryogenically liquefied, with obvious costs. Thus finding new techniques to convert gas into a liquid product is a valuable option.

Nowadays a main concern is the increasing atmospheric concentration of CO₂. In the recent past, it remained almost

constant at about 280 ppm until about two hundred years ago, when it started to grow in conjunction with the mounting exploitation of fossil fuels. At present, CO₂ concentration stands at 400 ppm, and consequently the power of the Earth's greenhouse effect has been enhanced.

An obvious way to cut down the emission of CO₂ is to substitute fossil fuels with renewable energy sources, which are CO₂ neutral but frequently intermittent, and to recycle CO₂ to produce value-added chemicals and fuels [2]. In fact, solar energy is quite abundant—about four orders of magnitude of the current energy consumption—but it needs to be stored and transported.

In this framework, the production of syngas (CO + H₂) from CO₂ by using solar energy can be a way to store intermittent renewable energy into the chemical production chain. Converting CO₂ into chemical fuels requires a source of hydrogen. If CH₄ is used, as in the so-called dry reforming reaction $\text{CH}_4 + \text{CO}_2 \rightarrow 2\text{CO} + 2\text{H}_2$, two main greenhouse gases are used. In addition, CH₄ can be eventually converted via gas-to-liquid chemistry into a high energy-density fuel. Biogas valorisation is an ideal application of such a technology,

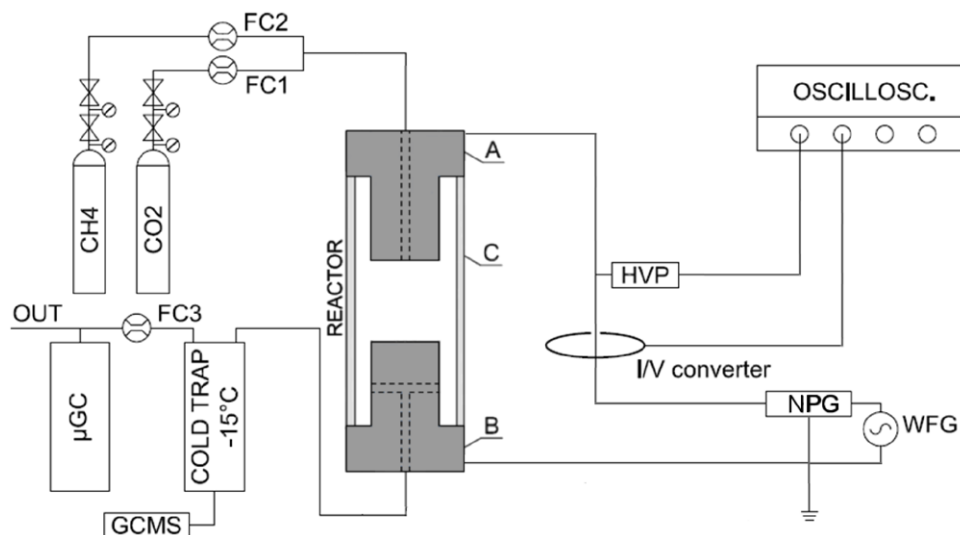


Figure 1. Schematic representation of the experimental setup. A: high-voltage electrode; B: grounded electrode; C: glass tube reactor; HVP: high voltage probe; NPG: nanosecond pulsed generator; WFG: wave-form generator; FC: mass flow controller/microGC: micro gas chromatograph; GCMS: gas chromatography–mass spectrometry instrument.

since renewable sources of methane, carbon dioxide and energy can be used to produce value-added chemicals and eventually liquid fuels by the Fischer–Tropsch process.

Dry reforming is a very endothermic reaction ($\Delta H_{298\text{ K}} = 247\text{ kJ mol}^{-1}$), since both CO_2 and CH_4 are quite stable molecules. Thermodynamic calculations [3] indicate that a temperature of at least 1000 °C is needed to get appreciable conversions. Low temperature values can be reached by using catalysts, but then the problem is their deactivation by carbon deposition.

Therefore, an attractive possibility is to consider the non-equilibrium properties of gaseous electrical discharges for channelling energy in the molecular dissociation rather than in heating the gas [4]. A further advantage of using plasma techniques to dissociate CO_2 and CH_4 is directly related to the storage of green electricity. Since discharges can be switched on and off quickly, plasma systems are suitable to be coupled with an intermittent electric power source, thus providing a flexible and scalable technology for storing renewable energy into chemical energy.

By far the most studied discharge is the dielectric barrier discharge (DBD), due to its simplicity and reliability [5]. When CO_2 and CH_4 are the feed gases, a DBD produces syngas and light hydrocarbons, but also liquid oxygenates [6, 7] and liquid hydrocarbons [8, 9]. Unfortunately, both the conversion rate and the global energy efficiency are low. To overcome these limitations, the synergy between plasma and the heterogeneous catalysis is currently being actively investigated [10]. A complementary route is to attempt different discharge configurations, such as corona [11], microwave (MV) [12], spark [13] and gliding-arc [14]. In this context, a repetitive pulsed excitation with a nanosecond scale pulse rise time and duration (NRP) appears to be a promising candidate due to its highly non-equilibrium nature [15]. In this paper we report on experiments carried out by an atmospheric pressure NRP discharge in a $\text{CH}_4\text{--CO}_2$ mixture, with a detailed analysis of the products, not limited to syngas only, which is very important to correctly define the energy efficiency. We present results on the reactant conversion, product selectivity and energy

efficiency, and compare them with available literature data relevant to other discharge types.

We find that the NRP energy efficiency is larger than the values of the DBD, corona and microwave discharges, and comparable to that of gliding arcs. Possible limiting factors to the efficiency increase are discussed.

2. Experimental methods

The experimental setup is shown in figure 1. The reactor is made of a quartz tube (internal diameter 10 mm, external diameter 13 mm), containing two brass discs (diameter 8 mm). The discharge in the plane-to-plane configuration occurs in an inter-electrode gap that can vary up to 10 mm.

The discharge is produced by a nanosecond-scale pulsed power supply (NPG 18/3500, Megaimpulse Ltd.), triggered by a wave-form generator (WFG) (33220A, Agilent Technologies Inc.). Discharge current and voltage values are measured by a I/V converter (CT-D-1.0, Magnelab) and a high-voltage probe (P6015A, Tektronix), respectively. I and V signals are recorded by a digital oscilloscope (WaveSurfer 104MXs-A, LeCroy). The pulse repetition rate is controlled by the WFG and ranges from 100 up to 3000 Hz.

Two mass flow controllers set the input flow; a third one, placed at the exit of a cold trap at -15 °C , records the output flow. The input flow is changed between 200 sccm and 600 sccm, which translates in a variation of the residence time in the discharge between 0.012 s and 0.036 s for a gap of 2.5 mm.

On-line gas detection is performed by using a gas-chromatograph (3000 Micro GC, Agilent Technologies Inc.). Helium, hydrogen, methane and carbon monoxide were measured by a Molesieve column with back-flush; carbon dioxide, ethane, ethylene, acetylene, propane and propyne by using a Plot U column. Standard compounds were used to calibrate the instrument. A small amount ($<0.5\%$) of pure helium was added to the reactant flux as an internal standard to accurately take into account possible variations of the

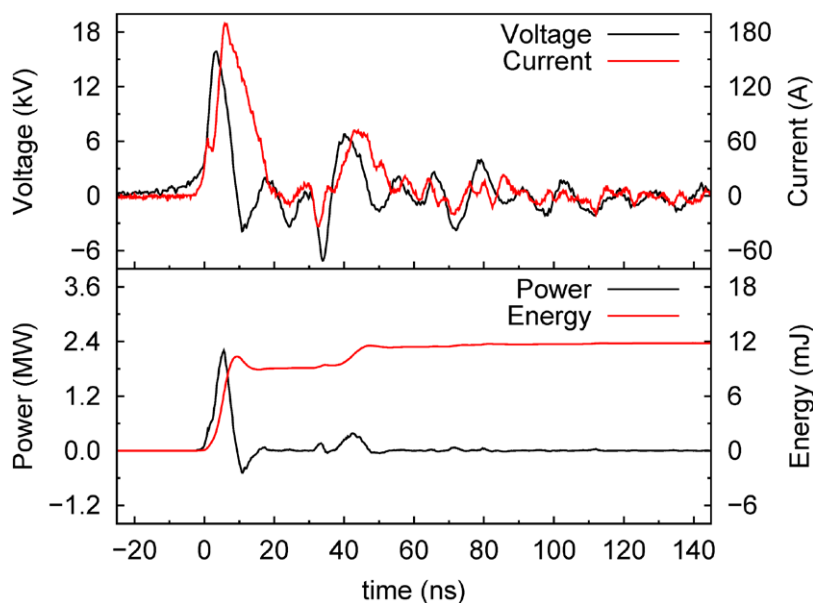


Figure 2. Voltage, current, instantaneous power, and energy for a 6 ns FWHM, 15.8 kV pulse.

response factor of the third mass flow meter. Compounds condensed in the cold trap were dissolved in acetonitrile and analysed using a GC-MS (Trace GC Ultra, Finningham). Water, the main liquid by-product, was estimated by the standard addition method with a Carbowax column. The quantitative measurement of water requires very long discharge runs in order to collect a sufficient amount; for this reason, we did not carry it out routinely. Solid carbon was collected from the reactor wall and characterised by scanning electron microscopy, FTIR and XPS spectroscopy. Carbon quantitative measurement is prevented by the impossibility to completely collect it.

2.1. Discharge power measurement

The discharge power measurement is a delicate issue when dealing with short voltage and current pulses. The time delay introduced by the acquisition system introduces a spurious phase shift between I and V , that in turn affects the power estimation. We measured this time delay, with the discharge off, by reducing to zero the time integral of the $I \times V$ product [16]. To this end, we maintained the same circuit configuration and reactor geometry, by filling the reactor with Freon-113 vapour to prevent breakdown. For a 2.5 mm gap, the time delay was estimated as (2.15 ± 0.09) ns. The instantaneous power is then calculated as the $I \times V$ product accounting for the spurious delay. The pulse energy is the time integral of the instantaneous power. Figure 2 shows an example of the recorded voltage and current signals. The instantaneous power and pulse energy are also shown.

2.2. Process characterisation

Quantities for process characterisation must be chosen accurately. Many parameters have been introduced in the literature to compare different discharges. Some authors consider

only the conversion of reactants, defining the conversion ability [12] or the energy efficiency [17] or the energy cost for converting CH_4 and CO_2 [18]. These choices are limiting, since not all the products are energetically useful, and therefore efficiency calculations based only on conversion substantially overestimate the efficiency and mask its trends as a function of discharge parameters. Tao *et al* [19] introduce specific energy and energy conversion efficiency (ECE), considering only H_2 and CO as products, while Zhu *et al* [18] calculate the energy cost for H_2 production. Also these quantities are incomplete, since other hydrocarbon products should be considered in the energy evaluation, especially if their selectivity is larger than 10%.

Following [20], we consider the ECE, defined as the ratio between the energy contained in the products and the sum of the energy of the converted reactants with the energy injected in the plasma. In the following we give the formulas for the quantities used in the paper. Setting:

- n_r^{in} and n_r^{con} as the input and converted moles of reactants r ;
- P and E as the power and energy of the discharge;
- Φ_r as the total flux of reactants;
- n_x as the number of moles of species x ;
- LHV_r and LHV_{pr} as the lower heating value of reactants and products.

We define the conversion of reactants (methane or carbon dioxide):

$$C_r = \frac{n_r^{\text{con}}}{n_r^{\text{in}}} \times 100; \quad (1)$$

the specific energy input (SEI), i.e. the average amount of energy injected in the plasma per unit volume:

$$\text{SEI} = \frac{P}{\Phi_r} \quad (\text{kJ dm}^{-3}); \quad (2)$$

the gaseous products selectivity:

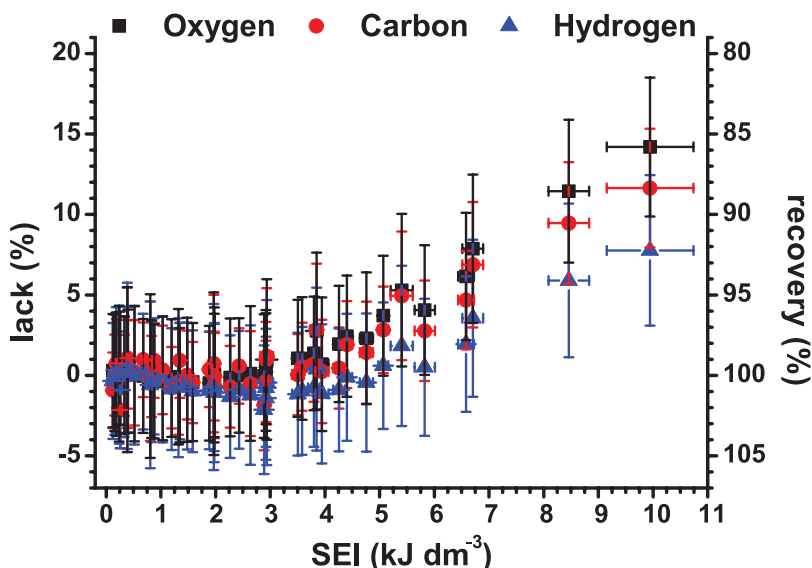
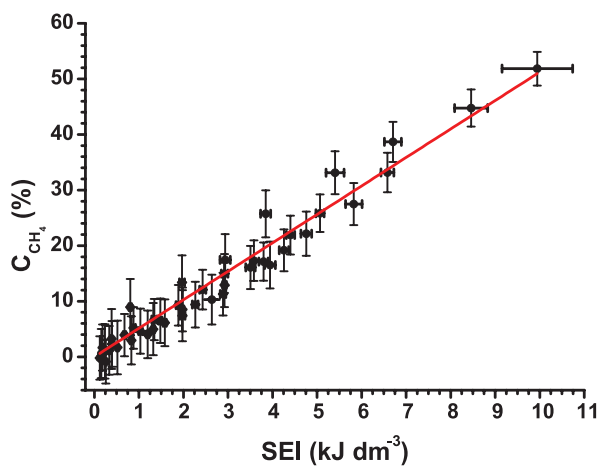
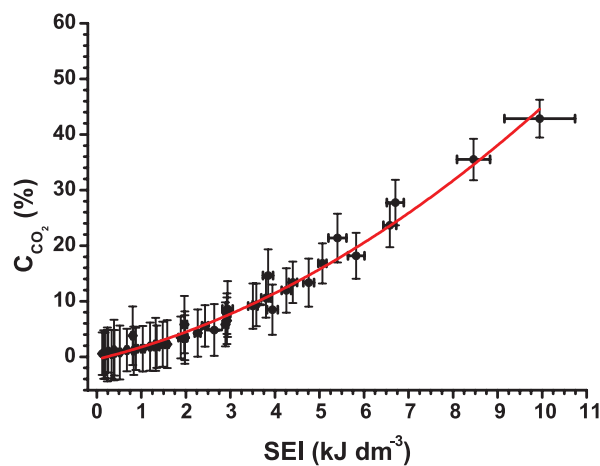


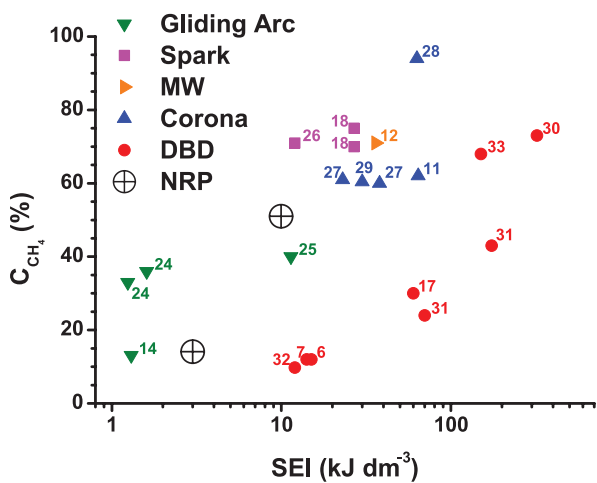
Figure 3. Mass balance as a function of the SEI. Lack is the missing percentage of a given element in the mass balance. Recovery is the percentage of a detected element with respect to the amount contained in the reactants.



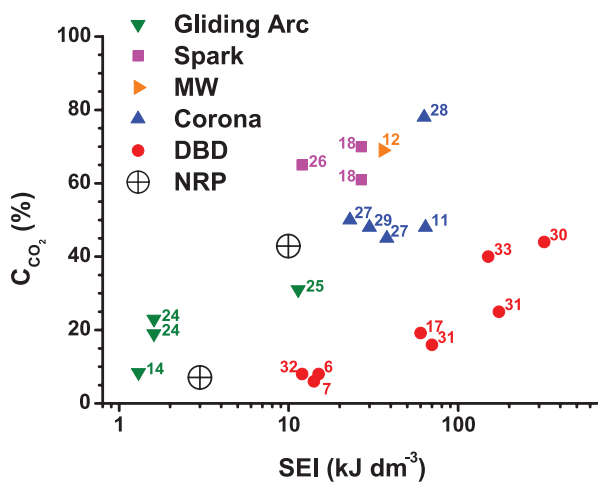
(a)



(b)



(c)



(d)

Figure 4. Conversion rates as a function of the SEI. Present data are reported in (a) and (b), while in (c) and (d) literature data for various discharges are compared. For simplicity, we show our results for two SEI values only. Numbers correspond to references.

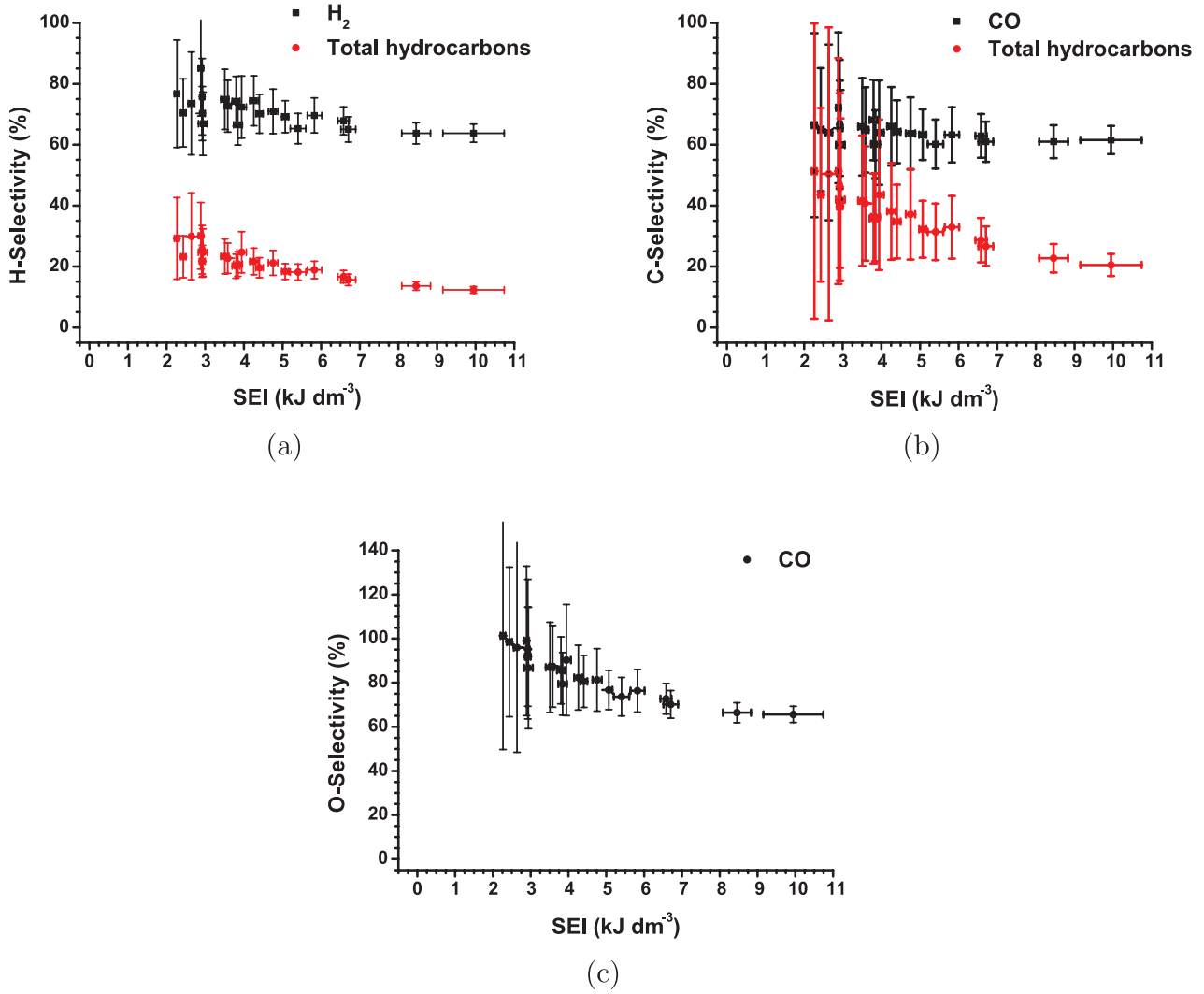


Figure 5. Selectivity. (a): with respect to hydrogen; (b): with respect to carbon; (c): with respect to oxygen.

$$\begin{aligned}
 S_{\text{H}_2} &= \frac{n_{\text{H}_2}}{2 n_{\text{CH}_4}^{\text{con}}} \times 100; \\
 S_{\text{CO}}^{\text{C}} &= \frac{n_{\text{CO}}}{n_{\text{CH}_4}^{\text{con}} + n_{\text{CO}_2}^{\text{con}}} \times 100; \\
 S_{\text{CO}}^{\text{O}} &= \frac{n_{\text{CO}}}{2 n_{\text{CO}_2}^{\text{con}}} \times 100; \\
 S_{\text{C}_x\text{H}_y}^{\text{C}} &= \sum_{x,y} \frac{x n_{\text{C}_x\text{H}_y}}{n_{\text{CH}_4}^{\text{con}} + n_{\text{CO}_2}^{\text{con}}} \times 100; \\
 S_{\text{C}_x\text{H}_y}^{\text{H}} &= \sum_{x,y} \frac{y n_{\text{C}_x\text{H}_y}}{4 n_{\text{CH}_4}^{\text{con}}} \times 100.
 \end{aligned} \quad (3)$$

in which the hydrocarbon selectivity is the sum over all the measured hydrocarbon products (total hydrocarbon); the ECE:

$$\text{ECE} = \frac{\text{LHV}_{\text{pr}}}{\text{LHV}_{\text{r}} + E} \times 100. \quad (4)$$

and, finally, the energy storage efficiency (ESE):

$$\text{ESE} = \frac{\text{LHV}_{\text{pr}} - \text{LHV}_{\text{r}}^{\text{con}}}{E} \times 100. \quad (5)$$

3. Results and discussion

The discharge has generally a glow structure, but its nature shows differences depending on the gap between the electrodes. For a gap of 2 mm, the presence of a few filaments was observed, while at a higher gap (8 mm), the filaments disappear and the discharge extends up to the quartz tube walls. For the latter configuration, we guess that carbon powder formation on the glass might increase the surface conduction and promote the surface discharge, thus changing the nature of the discharge itself. For this reason, we report only the results for a gap of 2.5 mm, where the higher stability allows to work in a wider range of pulse repetition rates. The conversion, selectivity and ECE/ESE have been calculated from measured products and are reported as a function of the SEI. The SEI is varied up to 10 kJ dm⁻³, by varying both the HV pulse repetition rate and the reactant flux. By changing Φ_{r} and P , such as SEI remains constant, we got similar results. The SEI upper limit is set by the difficulty of handling the experiment at low flux values. For the highest SEI of 10 kJ dm⁻³, we estimated the temperature of the reactor exhaust to be around 170 °C by using a thermocouple.

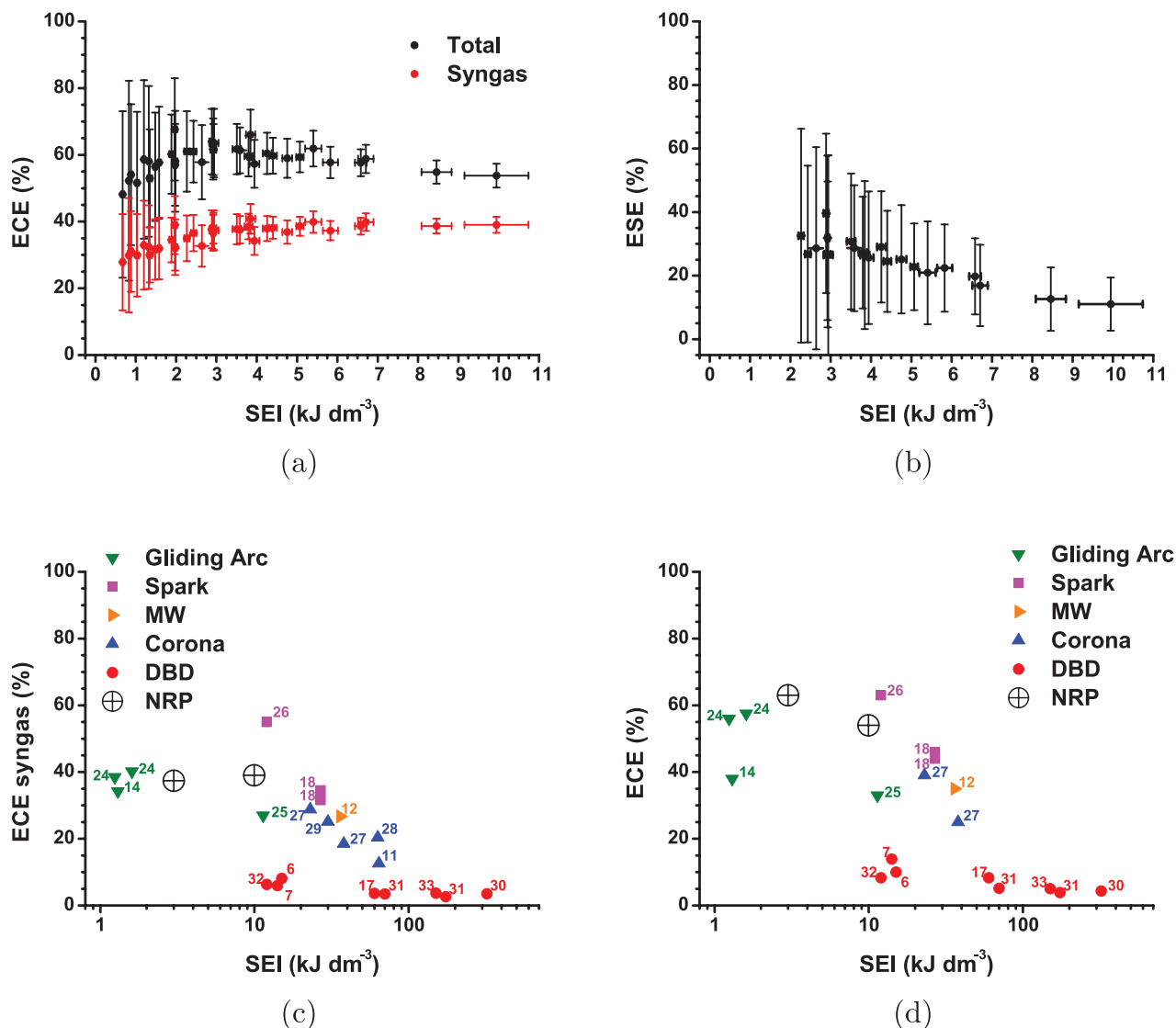


Figure 6. ECE and ESE as functions of SEI. Present data are shown (a) and (b), while in (c) and (d) a comparison with literature data for various discharge types is reported. For simplicity, we show our results for two SEI values only. Numbers correspond to references.

3.1. Mass balance

The mass balance, calculated from gaseous products data, is shown in figure 3. At SEIs lower than 3 kJ dm^{-3} , the recovery is total. At higher SEIs, the balance indicates that a significant amount of mass is not detected, and this behaviour increases with the SEI.

Oxygen is the species with the lower recovery; we guess this is due to water formation. Indeed, in a long discharge run at the $\text{SEI} = 6.5 \text{ kJ dm}^{-3}$, we have measured about 500 mg of water that fits quite well with the 600 mg calculated from the oxygen lack.

Carbon lack is due to the formation of carbon powder, which is dispersed throughout the reactor. Its analysis confirms the presence of C–C and C–H bonds, both aliphatic and aromatic.

3.2. Reactants conversion

The reactant conversion is shown in figures 4(a) and (b). Methane conversion is roughly linear with the SEI variation,

and its value is higher than for CO_2 conversion, similarly to what has been observed in other cold plasmas [21] and model calculations [22]. CO_2 , instead, shows a rather parabolic behaviour. The rationalisation of these results requires complex model calculations. We just note that, if we calculate the total conversion, $0.5 \text{ C}_{\text{CH}_4} + 0.5 \text{ C}_{\text{CO}_2}$, we find a non-linear behaviour that looks similar, although in a different SEI range to that measured in a coaxial DBD reactor and calculated by a zero-dimensional kinetic model [23].

In figures 4(c) and (d) we compare conversion values for different plasmas, whose values are calculated from recent literature. At higher SEIs the conversion increases for all the discharges [24–33]. DBDs are easy to develop and have been well-studied, but they show low performance. Corona, another well-known discharge, has a better performance, but the discharge volume is very small in comparison to others. Microwave discharges have good performance and large volumes, but require complex systems. Gliding, spark and NRP have similar performances.

3.3. Product selectivity

The selectivity, as defined in (3), is reported in figure 5. Analysis of the discharge effluents shows that the main products are H₂ and CO. Their selectivity with respect to hydrogen and carbon are almost constant with SEI variation. The selectivity of CO with respect to oxygen shows an higher decrease, which we attribute to water formation. For hydrocarbons, the selectivity with respect to both hydrogen and carbon slightly decreases with the SEI.

The most abundant hydrocarbon product is acetylene, but other alkynes, such as methylacetylene, are also detected. Since in DBD reforming the main product is ethane [6], this difference suggests a different initial radical abundance, i.e. in NRP CH prevails on CH₃, while in a DBD the reverse occurs. This hydrocarbon distribution is more similar to that found in gliding arc or spark discharges, with a prevalence of unsaturated byproducts [17, 26].

At low SEI, hydrogen, CO and light hydrocarbons are the main products. Increasing the discharge power, water and carbon powder become important products.

3.4. Energy efficiency

We have selected ECE to evaluate the process efficiency, since this quantity correctly accounts for the amount of chemical energy stored in the products. In figure 6(a), the ECE is plotted versus the SEI, both for syngas only and for all the gaseous products (carbon powder is still excluded). The difference between the two ECE values suggests that the energy stored in products other than syngas is not negligible. The energy efficiency reaches a plateau at about 3 kJ dm⁻³ and then starts to decrease slowly; this is likely due to a competing production of water and carbon. This appears to be a limiting factor that prevents the efficiency from increasing as a function of the SEI.

Considering other cold plasma techniques, NRP has better performance with respect to DBDs, MW and corona discharges, and one similar to gliding and spark discharges. We finally observe that the best efficiency at low SEI values, and the decrease of efficiency at high SEI, is a general feature of all the kinds of discharges. Therefore we guess that water and carbon formation might be a general limiting factor of the plasma treatment, occurring in different SEI ranges according to the energy deposition mechanisms of the various discharge technologies.

ECE expresses the efficiency of the total process, but it does not give information on the efficiency of energy storing. The energy efficiency in energy storage can be calculated as the difference of LHV between the products and reactants divided by the discharge energy (see (5)). It is shown in figure 6(b). The best performance we achieve is about 30%.

In figures 6(c) and (d) we compare our ECE values with literature data. The latter have been calculated by using the products reported in each reference.

In addition to energy, also CO₂ can be stored, since a fraction of carbon contained in the products derives from CO₂.

4. Conclusions

The main conclusions we can draw are as follows:

- (i) The energy efficiency of the NRP treatment is among the highest compared to other kinds of discharge. Its value is sufficiently high as to justify further research to improve it.
- (ii) Both CH₄ and CO₂ conversions increase as a function of SEI. However, the selectivity towards syngas decreases; this is likely due to a competing production of water and carbon powder.
- (iii) The bare discharge is not totally selective towards syngas.

To improve the process one should first of all have the final target clear in mind: for example, the syngas production, liquid fuels production, energy storage, and CO₂ disposal.

The step forward must seek selectivity improvements and/or play with discharge parameters [6], or with heterogeneous catalysis process integration [17].

From the point of view of energy efficiency, a key point seems to be finding a way to inhibit water formation (note that the energy content of carbon powder can be in principle re-utilised, thus increasing the global energy efficiency). For this purpose, we should first of all understand water-formation mechanisms. From the present results, however, we already understand that working at low SEI values is advantageous, and we might envisage a cascade of low-SEI discharge stages as a possible avenue to pursue.

As a pure energy storage technique, the efficiency appears to be still too low as compared, for example, with storage in H₂ by electrolysis, which reaches efficiencies in the order of 80–90%.

The advantages of plasma reforming of CH₄ + CO₂ must then be looked for in a multi-target application concept, in which value-added chemicals conversion, energy storage and CO₂ disposal are simultaneously achieved. Biogas treatment appears to be an ideal application of plasma reforming.

Acknowledgments

This work has been supported by the project ENAM funded by Provincia Autonoma di Trento in cooperation with CNR-IMCB (Italy). We thank N Laidani (FBK Trento) and N Bazzanella (University of Trento) for supporting us with XPS and scanning electron microscopy measurements, respectively.

References

- [1] 2014 BP Statistical Review of World Energy <http://www.bp.com/en/global/corporate/energy-economics/statistical-review-of-world-energy.html>
- [2] Perathoner S and Centi G 2014 *ChemSusChem* **7** 1274–82
- [3] Nikoo M K and Amin N 2011 *Fuel Process. Technol.* **92** 678–91
- [4] Chu P K and Lu X (ed) 2013 *Low Temperature Plasma Technology: Methods and Applications* (Boca Raton, FL: CRC Press)
- [5] Chirokov A, Gutsol A and Fridman A 2005 *Pure Appl. Chem.* **77** 487–95

- [6] Martini L M, Dilecce G, Guella G, Maranzana A, Tonachini G and Tosi P 2014 *Chem. Phys. Lett.* **593** 55–60
- [7] Scapinello M, Martini L M and Tosi P 2014 *Plasma Process. Polym.* **11** 624–8
- [8] Scarduelli G, Guella G, Mancini I, Dilecce G, De Benedictis S and Tosi P 2009 *Plasma Process. Polym.* **6** 27–33
- [9] Scarduelli G, Guella G, Ascenzi D and Tosi P 2011 *Plasma Process. Polym.* **8** 25–31
- [10] Kameshima S, Tamura K, Ishibashi Y and Nozaki T 2015 *Catal. Today* **256** 67–75 (plasmas for enhanced catalytic processes (ISPCEM 2014))
- [11] Yang Y 2002 *Ind. Eng. Chem. Res.* **41** 5918–26
- [12] Zhang J Q, Zhang J S, Yang Y J and Liu Q 2003 *Energy Fuels* **17** 54–9
- [13] Shapoval V, Marotta E, Ceretta C, Konjević N, Ivković M, Schiorlin M and Paradisi C 2014 *Plasma Process. Polym.* **11** 787–97
- [14] Tu X and Whitehead J C 2014 *Int. J. Hydrog. Energy* **39** 9658–69
- [15] Iza F, Walsh J and Kong M 2009 *IEEE Trans. Plasma Sci.* **37** 1289–96
- [16] Takashima K, Zuzeeq Y, Lempert W R and Adamovich I V 2011 *Plasma Sources Sci. Technol.* **20** 055009
- [17] Tu X and Whitehead J 2012 *Appl. Catal. B: Environ.* **125** 439–48
- [18] Zhu B, Li X S, Shi C, Liu J L, Zhao T L and Zhu A M 2012 *Int. J. Hydrog. Energy* **37** 4945–54 (optimization approaches to hydrogen logistics)
- [19] Tao X, Bai M, Li X, Long H, Shang S, Yin Y and Dai X 2011 *Prog. Energy Combust.* **37** 113–24
- [20] Lotfalipour R, Ghorbanzadeh A M and Mahdian A 2014 *J. Phys. D: Appl. Phys.* **47** 365201
- [21] Rico V J, Hueso J L, Cotrino J and González-Elipé A R 2010 *J. Phys. Chem. A* **114** 4009–16
- [22] Snoeckx R, Aerts R, Tu X and Bogaerts A 2013 *J. Phys. Chem. C* **117** 4957–70
- [23] Snoeckx R, Zeng Y X, Tu X and Bogaerts A 2015 *RSC Adv.* **5** 29799–808
- [24] Bo Z, Yan J, Li X, Chi Y and Cen K 2008 *Int. J. Hydrog. Energy* **33** 5545–53
- [25] Indarto A, Choi J W, Lee H and Song H K 2006 *Energy* **31** 2986–95
- [26] Shapoval V and Marotta E 2015 *Plasma Process. Polym.* **12** 808–16
- [27] Ghorbanzadeh A, Lotfalipour R and Rezaei S 2009 *Int. J. Hydrog. Energy* **34** 293–8
- [28] Li M W, Xu G H, Tian Y L, Chen L and Fu H F 2004 *J. Phys. Chem. A* **108** 1687–93
- [29] Li M W, Liu C P, Tian Y L, Xu G H, Zhang F C and Wang Y Q 2006 *Energy Fuels* **20** 1033–8
- [30] Wang Q, Yan B H, Jin Y and Cheng Y 2009 *Plasma Chem. Plasma Process.* **29** 217–28
- [31] Song H, Lee H, Choi J W and Na B K 2004 *Plasma Chem. Plasma Process.* **24** 57–72
- [32] Goujard V, Tatibouet J M and Batiot-Dupeyrat C 2011 *Plasma Chem. Plasma Process.* **31** 315–25
- [33] Zhang K, Kogelschatz U and Eliasson B 2001 *Energy Fuels* **15** 395–402